

Polydopamine Meets Solid-State Nanopores: A Bioinspired Integrative Surface Chemistry Approach To Tailor the Functional Properties of Nanofluidic Diodes

Gonzalo Pérez-Mitta,[†] Jimena S. Tuninetti,[†] Wolfgang Knoll,[‡] Christina Trautmann,[§] María Eugenia Toimil-Molares,[§] and Omar Azzaroni^{*,†}

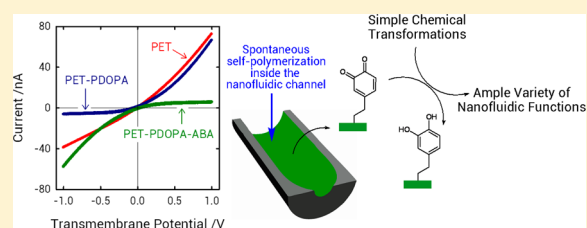
[†]Instituto de Investigaciones Fisicoquímicas Teóricas y Aplicadas (INIFTA), Universidad Nacional de La Plata – CONICET, CC 16 Suc. 4, (1900) La Plata, Argentina

[‡]Austrian Institute of Technology GmbH, Donau Strasse 1, Vienna, Austria

[§]GSI Helmholtzzentrum für Schwerionenforschung GmbH, Darmstadt, Germany

Supporting Information

ABSTRACT: The ability to modulate the surface chemical characteristics of solid-state nanopores is of great interest as it provides the means to control the macroscopic response of nanofluidic devices. For instance, controlling surface charge and polarity of the pore walls is one of the most important applications of surface modification that is very relevant to attain accurate control over the transport of ions through the nanofluidic architecture. In this work, we describe a new integrative chemical approach to fabricate nanofluidic diodes based on the self-polymerization of dopamine (PDOPA) on asymmetric track-etched nanopores. Our results demonstrate that PDOPA coating is not only a simple and effective method to modify the inner surface of polymer nanopores fully compatible with the fabrication of nanofluidic devices but also a versatile platform for further integration of more complex molecules through different covalent chemistries and self-assembly processes. We adjusted the chemical modification strategy to obtain various configurations of the pore surface: (i) PDOPA layer was used as primer, precursor, or even responsive functional coating; (ii) PDOPA layer was used as a platform for anchoring chemical functions via the Michael addition reaction; and (iii) PDOPA was used as a reactive layer inducing the metallization of the pore walls through the in situ reduction of metallic precursors present in solution. We believe that the transversal concept of integrative surface chemistry offered by polydopamine in combination with the remarkable physical characteristics of asymmetric nanopores constitutes a new framework to design multifunctional nanofluidic devices employing soft chemistry-based nanofunctionalization techniques.



INTRODUCTION

The use of asymmetric solid-state nanopores to construct functional nanofluidic devices represents major research efforts in the rapidly developing area of nanofluidics.^{1–4} Part of the appeal of nanofluidic diodes relies on their interesting ion-transport characteristics, which closely resemble the ion selectivity and ion current rectification properties of biological ion channels.^{5,6} One of the key factors that determine the rectifying characteristics of the asymmetric nanopores is the nanoscale control over the surface properties of the pore walls.⁷ Experimental⁸ and theoretical⁹ results have demonstrated that the rectifying properties of asymmetric nanopores emerge due to a synergy of the entropic driving force caused by the channel asymmetry and the electrostatic effects due to the fixed charges on the pore wall.^{10–12} During the past decade, increase in awareness and understanding of these factors that govern the responsive behavior of nanopore devices gave rise to a broad variety of nanofluidic architectures responding to external stimuli such as pH,¹³ specific ions,¹⁴ temperature,¹⁵ biomolecules,¹⁶ electric field,¹⁷ pressure,¹⁸ and light.¹⁹ The key element

for these ionic nanoporous devices is the possibility of triggering changes in the surface charge of the pore walls in the presence of a given environmental stimulus, which ultimately leads to changes in the type of ions and the concentration of ions inside the nanopore. Consequently, finding new avenues to manipulate the surface chemistry and the nature of the fixed charges of asymmetric nanopores is of paramount importance to gain control over the ion transport through the fluidic device and further expand the potentialities of these nanosized systems.

During the past 2 decades, a number of macromolecular and supramolecular techniques have been developed to modify surfaces and confer them functional features, for example, layer-by-layer assembly, Langmuir–Blodgett deposition, and self-assembled monolayers. In spite of having been applied successfully to certain surfaces, all these techniques have a common problem: *they are not transferable to all types of*

Received: February 13, 2015

Published: April 16, 2015

materials. Normally, these methods are restricted to surfaces with certain characteristics. For example, the electrostatic self-assembly is restricted to surfaces that have a charge of a determined sign or thiol chemistry is not compatible with polymer surfaces. Because of this problem, there is a great demand for new approaches that lead toward more generalized techniques to functionalize surfaces. Consequently, devising strategies that enable the integration of different surface chemistries in the same pore surface is one remaining challenge in nanofluidic research. In this context, polydopamine derivatives seem to have attained this well-coveted goal. Polydopamine, a polymer formed by 3,4-dihydroxy-L-phenylalanine (dopamine), is synthesized spontaneously by an oxidative process. This process occurs under basic conditions and in the presence of an oxidant and occurs both in solution and over surfaces. In 2007 Messersmith and co-workers²⁰ proposed a number of ways to synthesize and use polydopamine (PDOPA) to modify a large variety of surfaces, and thereafter it has been thoroughly studied by numerous groups.

Despite the fact that the chemical composition of the PDOPA has not been fully elucidated, certain functional groups are known to be present in the polymer, like catechol, imine, and amines. This is important because the chemistry of these groups makes it possible to modify further a layer of PDOPA to obtain surfaces with improved characteristics for specific applications. A type of reaction that has been used to modify PDOPA layers is the Michael addition, which allows grafting nucleophilic species such as primary amines and thiols to the polymer.^{20–23} Moreover, another reaction that has been used in this case to obtain metal–polymer hybrid materials is the reduction of metal ions during and after the polymerization of the PDOPA making use of the reactive catechol groups present in the polymer.^{24,25} Although the PDOPA has been extensively studied in a broad variety of applications, the use of PDOPA as a “universal primer” to develop responsive nanofluidic devices remains fully unexplored. Because of the versatility of the PDOPA to polymerize over virtually any surface and its ease to be chemically modified, this polymer represents an ideal building block to be combined with nanofluidic devices to improve the control over the transport phenomena.

In a similar vein, another feature that previous works in this field have in common is the configuration of etched single ion-track nanopore dimensions and tip size through chemical-etching strategies. The irreversible nature of the etching protocol shows that nanopores need to be discarded if longer etching times result in too large pore diameters that do not exhibit good rectification properties. In this context, it would be highly desirable to develop a facile technique to modify not only the chemistry but also the tip size and geometry of nanopores after the construction. Herein, we report a new and versatile approach to confer multiple functional properties to solid-state nanochannels by using self-polymerized dopamine under different scenarios. We show that it is possible to obtain pH-responsive ionic diodes with enhanced rectification properties from poorly rectifying asymmetric nanochannels by exploiting the dimensional and surface chemical changes taking place during PDOPA growth inside the pore. Moreover, we have exploited the chemistry of PDOPA to tailor the nanochannel properties as a proof of concept of the feasibility of the polymeric layer to develop fluidic nanodevices. To do so, we applied two different protocols. First, 3-aminobenzylamine was chemically grafted to the PDOPA by means of a Michael addition reaction, and second, we have used the reactive

catechol groups of the PDOPA to reduce gold to obtain a hybrid material constituted of PDOPA metallized with gold nanoparticles. Then the gold surface was subsequently modified with thiolate self-assembled monolayers bearing quaternary amino groups.

■ MATERIALS AND METHODS

Dopamine (DOPA), HAuCl_4 , and 3-aminobenzylamine (ABA) were purchased from Sigma-Aldrich (St. Louis) and used as received. Poly(ethyleneterephthalate) (PET) foils (Hostaphan RN 12, Hoechst), 12 μm , were irradiated at GSI Helmholtzzentrum für Schwerionenforschung GmbH (Darmstadt, Germany) with swift heavy ions (Au^{+25}), having energy of ~ 2.2 GeV. For the surfactant-assisted etching, the anionic surfactant Dowfax 2A1 from Dow Chemical was used. The *N,N,N*-trimethyl(3-mercaptopropyl)-ammonium chloride was synthesized as described in the literature.²⁶

Chemical Etching. PET foils irradiated with a single heavy ion were etched using a surfactant-assisted technique which conferred them a highly tapered “bullet-like” shape.²⁷ This etching was carried out in an electrochemical cell that separates both sides of the foil. One side of the cell was filled with etching solution, 6 M NaOH, while the other was filled with etching solution and surfactant, 6 M NaOH and 0.04% Dowfax 2A1. Before the etching, foils were irradiated with ultraviolet (UV) light for 2 h on the etching side only. The total etching time was either 6.5 or 8.0 min at a temperature of 60 °C, depending on the targeted rectification rate. There is considerable rectification at an etching time of 6.5 min, but then it decreases rapidly at higher etching times.²⁸

Conductivity Measurements. I–V characteristics were measured using a potentiostat, Reference 600 from Gamry, with a four-electrode setup in which the current flows between the working electrode and the counter electrode and the voltage is measured between two Ag/AgCl reference electrodes across the membrane. The potential is swept between 1 and –1 V with a scan rate of 0.1 V/s and a step size of 0.01 V. All the experiments were made using 0.1 M KCl solutions. The measurements at different pH values were performed without adding any buffer solution but adding dropwise solutions of HCl and NaOH. The counter electrode is always placed at the large opening base of the nanopore.

Rectification Rate. To compare all the results, a rectification rate (f_{rec}) must be defined. f_{rec} is defined as the quotient between the currents at 1 and –1 V. The current in the denominator is always the one with lower conductance. If the current in the nominator is negative, the result is multiplied by –1 so that a positive rectification rate is associated with a positive surface charge and a negative rectification with a negative surface charge.

Polymerization of Dopamine (DOPA). A 10 mM DOPA solution was left in contact with the PET foil at pH 8.5 (adjusted with 0.1 M Tris buffer) for 2 h. Potassium chloride was added up to a concentration of 0.1 M to conduct conductivity measurements during the formation of the PDOPA on the nanochannel walls.

Chemical Grafting of PDOPA. Using a Michael addition reaction, the PDOPA was modified with 3-aminobenzylamine (ABA).²¹ PDOPA nanochannels were left in a 2 mg/mL ABA solution for 72 h (pH 8.5 was adjusted with 0.1 M Tris buffer).

Electroless Preparation of Gold Coatings. Exposed catechol groups of the PDOPA layer were used as reducing agents. PDOPA-modified PET foils were left overnight in a 5 mM HAuCl_4 solution to obtain hybrid Au nanoparticle (NP)/PDOPA layer. To corroborate our procedure, we carried out two sets of experiments. First, UV–vis spectroscopy was used to monitor the appearance of the typical plasmonic features of gold NPs after the metallization step. The measurements were made using a Lambda 35 UV–vis spectrometer from Perkin-Elmer.

Contact Angle Measurements. Contact angles were measured using a Ramé-Hart contact angle system (Model 290) at 25 °C. In each measurement, a 2 μL droplet of water was dispensed onto the surface of the PET membrane. The average contact value was obtained at seven different positions of the same membrane.

RESULTS AND DISCUSSION

The dual role of PDOPA as a building block capable of altering the chemical and dimensional properties of the nanopores was demonstrated using a nanochannel displaying scarce rectification properties as a consequence of the larger tip size obtained after prolonged etching times (8 min at 60 °C). After characterizing the initial I–V response, the single pore-containing foil was washed with Milli-Q water and then put again in the conductivity cell with a solution of dopamine in Tris buffer (pH 8.5). The polymerization reaction starts immediately under these conditions. To follow the closing of the pore tip during the polymer growth on the pore walls, the transmembrane ionic current was measured as a function of time (Figure 1). This experiment allowed us to roughly

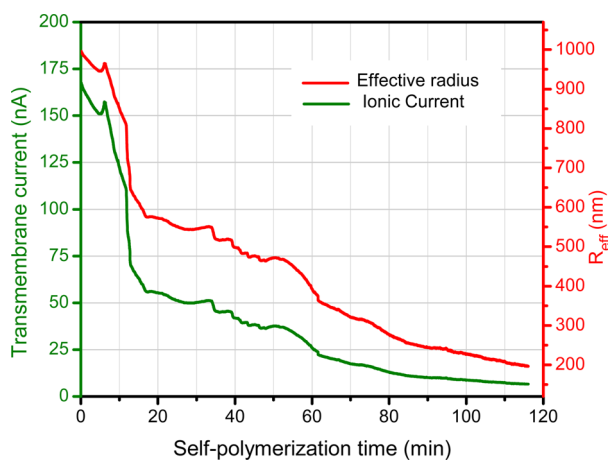


Figure 1. Transmembrane ionic current measured during the formation of the polydopamine layer on the nanochannel surface. It is shown that the pore tip is not blocked even after 2 h of polymerization.

estimate the effective radius of the nanochannel as the polymerization proceeded inside the pore. This effective radius R_{eff} is defined as the radius of a cylindrical pore having the same conductance G as the measured nanochannel. The R_{eff} was calculated using a typical conductivity equation,²⁹

$$R_{\text{eff}} = \sqrt{\frac{GL}{\kappa\pi}} \quad (1)$$

where L is the length of the channel (in our case 12 μm), G is the conductance of the channel, and κ is the specific conductance of the electrolyte. It can be seen in Figure 1 that there is a rapid decrease in the R_{eff} during the first 15 min. After this period, the polymerization rate within the pore decreased. The final regime lasted for more than 30 min without observing effective closure of the pore (Figure 1). The surface properties of PET films were examined before and after dopamine polymerization by contact angle (CA) measurements. The results of the CA measurements showed that the PDOPA polymerization led to a visible change of the surface wettability from 80° to 65° (see Supporting Information for details), thus indicating change in the surface chemical composition.

As expected, the I–V curve of the nanochannel after the polymerization showed lower values of transmembrane ionic currents as a consequence of the reduced tip size resulting from the PDOPA growth. However, the nanochannel displays a

marked increase in rectification rate (f_{rec}) from 2 to 10 after the PDOPA polymerization took place (Figure 2). A difference between the initial current in Figure 1 and the corresponding current in Figure 2B can be seen. This difference was found to be caused by the higher pH of the polymerization solution and also by a slight shift between the potentials of the reference electrodes used during the polymerization.

Up to date, the majority of the protocols to obtain nanofluidic diodes relied on bottom-up approaches in which the geometrical features that are responsible for the rectification of the ionic current are obtained by strict control over the variables during the fabrication of the channels. These variables include the etching time, temperature, or the transmembrane potential.^{30–33} By using only this approach, it is almost impossible to regain a non-ohmic, diode-like behavior after certain tip diameter of the asymmetric nanochannel is exceeded. Here, we used a new approach using the self-polymerization of dopamine to occlude the nanochannel in a very controlled manner not only to reduce the size of the channel but also to increase the rectification properties of the nanofluidic device. In this example, self-polymerization of PDOPA permitted drastic reduction of the effective radius to 20% of the original diameter, without blocking the passage of ions through the membrane. These results make the technique very attractive because it provides a protocol to obtain nanodevices from channels or pores of larger diameters. Theoretically, it should be possible to scale this procedure to channels with diameters on the order of micrometers. Future work will be done to elucidate this issue.

Next, the responsive behavior of the PDOPA-modified nanochannels as a function of pH was tested. Recently, Zhou and co-workers demonstrated that the presence of amine and phenolic hydroxyl groups confer PDOPA ampholytic or zwitterionic properties.³⁴ With this idea in mind we explored the use of PDOPA as a zwitterionic layer capable of controlling the nature of the surface charges on the pore walls, and therefore the rectification of the nanochannel by adjusting the pH of the electrolyte solutions (Figure 3a). The behavior of the system was studied in the $2 < \text{pH} < 12$ range (Figure 3b). Within this range, the rectification varied from positive to negative values, thus indicating variation from anion selectivity to cation selectivity (Figure 3c). When the I–V curves at different pH values were measured, a region within the $4.5 < \text{pH} < 6.4$ range in which $|f_{\text{rec}}| \sim 1$ was observed. This observation corresponds to ohmic behavior that in turn corresponds to the absence of net surface charge, that is, an “isoelectric” region (Figure 3c).

The modification of the nanochannel with PDOPA conferred the fluidic device pH responsiveness due to the capacity of the polymer layer to bear both negative and positive charges depending on the pH conditions. The rectification rates under alkaline conditions were larger than those observed in acidic solutions. Consequently, it can be proposed that the positive surface charge density at lower pH is smaller than the negative one at higher pH. This feature has been recently observed by Ball and co-workers, who measured the zeta potential of dopamine–melanin films under different pH conditions.³⁵ These authors proposed that quinone–imines and catechol groups present in the polymer are responsible for the negative charges in alkaline conditions, whereas at lower pH values the positive charges could arise from indol groups present in the polymer. In our experiment, a region of pH between 4.5 and 6.4 was found for which the net surface charge density was

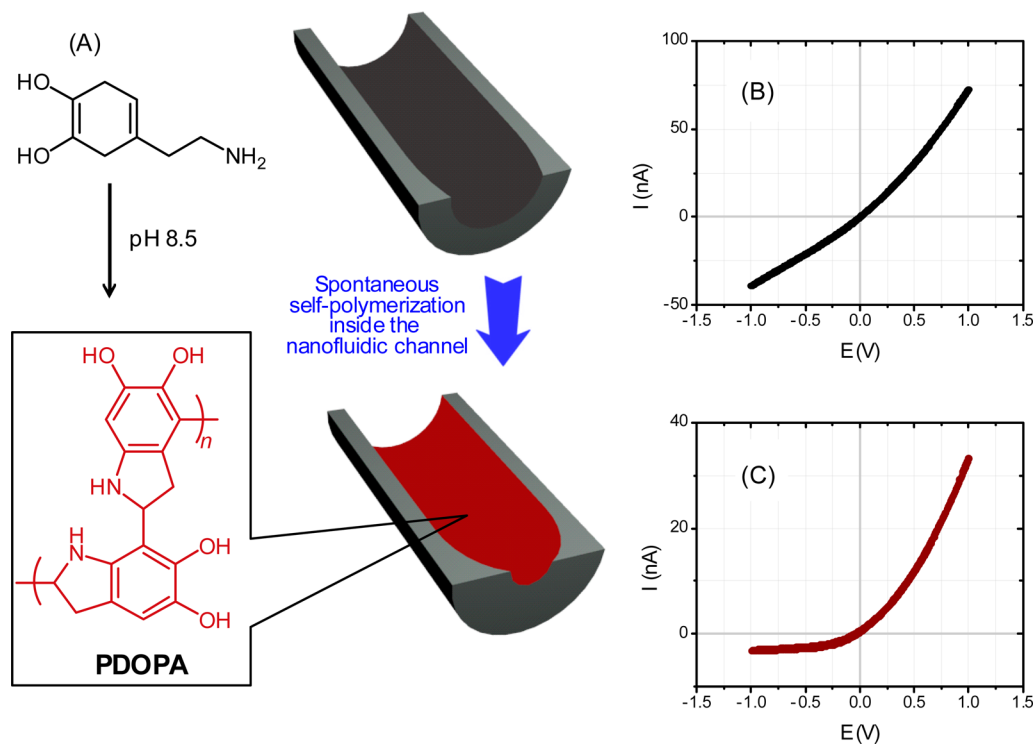


Figure 2. (A) Scheme showing the formation of the PDOPA layer on the pore walls. I–V characteristics of the nanochannel before (B) and after (C) the polymerization.

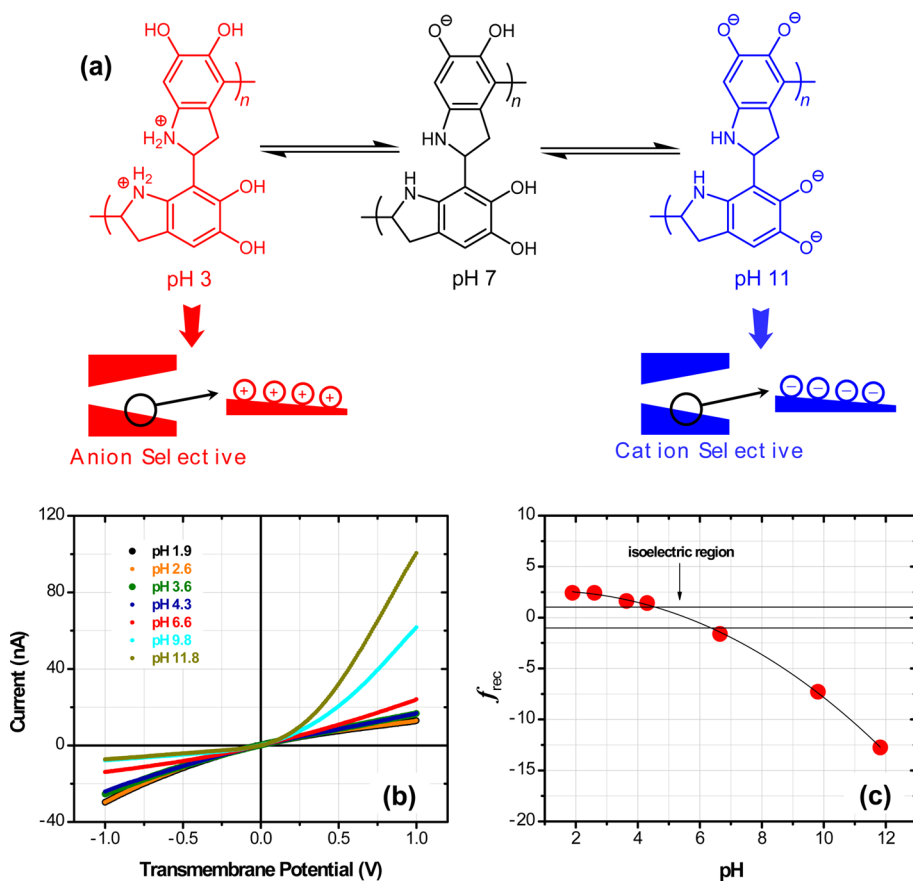


Figure 3. (a) Chemical equilibrium associated with the pH-dependent zwitterionic behavior of PDOPA. (b) I–V characteristics of a PDOPA-modified nanochannel under different pH conditions. (c) Rectification rate (f_{rec}) as a function of pH. It can be seen that the zwitterionic nature of polydopamine leads to the rectification reversal below and above the isoelectric region ($4.5 < \text{pH} < 6.4$). Lines were included to guide the eye.

supposed to be zero due to the lack of current rectification (Figure 3c). An interesting point to remark is that the value for the isoelectric point (IP) of the PDOPA reported by Ball et al.³⁶ using our same experimental conditions was about 4, which is close to our values. To be more precise, the isoelectric region in our nanopore system is slightly shifted toward higher pH values, as compared with those obtained in PDOPA particles. This observation could be attributed to charge regulation effects.³⁷ It has been shown that in the case of polymers confined in solid-state nanopores the degree of polymer charge is largely affected by charge regulation and nanoconfinement effects.³⁷ Consequently, charge regulation effects have a strong impact on acid–base equilibrium. In most cases, the acid–base equilibrium is displaced toward uncharged or less charged configurations to minimize the local electrostatic repulsions in the system. This mechanism controls the net charge of the confined polymer film, which is different from that expected in free solution or even on a particle surface. In our case, the shift toward higher pH values indicates that PDOPA layers when confined in a nanopore require more alkaline conditions to become negatively charged.

Then we exploited the chemical richness of PDOPA layer to attain the covalent grafting of functional groups through the Michael addition reaction of primary amines. As a proof of concept, 3-aminobenzylamine (ABA) was used as reagent, mainly because it bears a second protonable amine group that would reverse the direction of the rectification after the covalent integration in the PDOPA layer (Figure 4A). To accomplish full modification, PET/PDOPA foils must be immersed in a 2 mg/mL ABA solution (pH 8.5 adjusted with 0.1 M Tris buffer) for 5 days. Wetting measurements revealed

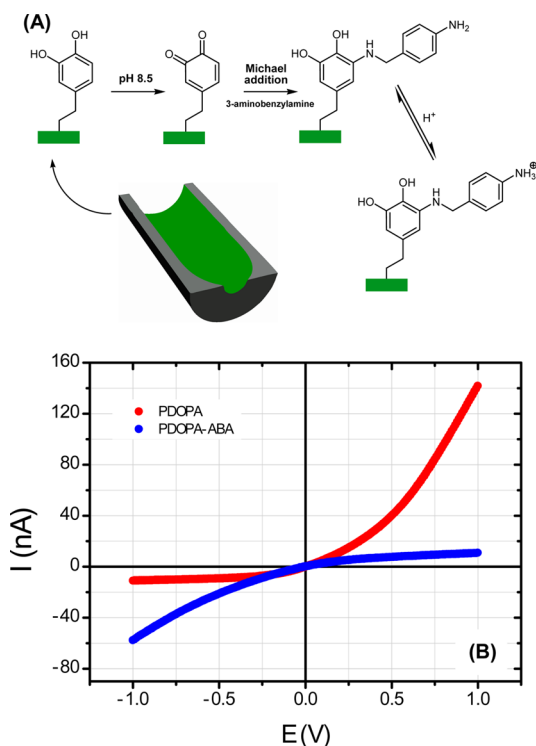


Figure 4. (A) Scheme showing the covalent grafting of 3-aminobenzylamine on the PDOPA layer via the Michael addition reaction. (B) I–V characteristics of the PDOPA-coated nanochannel prior to (red trace) and after (blue trace) grafting 3-aminobenzylamine. I–V plots were measured in 0.1 M KCl (pH 5).

that the modification of the PDOPA layer via Michael addition of 3-aminobenzylamine led to changes in surface wettability from 65° to 56°, thus evidencing changes in the chemical identity of the surface (see Supporting Information for details).

As expected, I–V characteristics of PDOPA nanochannels modified with ABA through the Michael addition reaction exhibited an inversion of the rectification direction (Figure 4B), leading to anion selectivity as a consequence of the positive surface charges introduced by the grafted primary amines. These experiments illustrate the versatility of the PDOPA layer in combination with the Michael addition reaction for tailoring the surface chemistry of the pore walls through the integration of predefined functional groups. Consequently, a large variety of robust functional nanosystems can be conceived using widely available primary amines.

Finally, we explored the dual role of PDOPA as a primer/precursor for the metallization of solid-state nanopores. Nanopore metallization is a key determining step in different nanopore-based technologies. To this end, techniques like ion sputtering³⁸ or electroless metallization have been previously employed to dress the pore walls with a thin metal layer. In particular, gold metallization of nanopores via electroless deposition was formerly introduced by the Martin group³⁹ as an intermediate step for further modification of the pore walls with self-assembled monolayers. This procedure enables the direct incorporation of functional elements into the inner pore walls; however, the gold-plating step requires careful control of the experimental conditions to avoid the blocking of the pore tip. That is why it is highly desirable to design alternative strategies enabling the facile metallization of the inner pore wall by directly exploiting the chemical functional groups already existing at the PDOPA-modified nanochannel wall. The application of PDOPA in metallization processes on planar surfaces was first proposed by Lee et al.²⁰ who demonstrated that catechol groups in the PDOPA layer can reduce metal ions in solution.

In our case, HAuCl_4 was used to form a colloidal gold–PDOPA composite layer on the pore walls. This was achieved by immersing the pore-containing PDOPA-modified foil in a 5 mM HAuCl_4 solution buffered at pH 8.5 (Tris) to shift the equilibrium toward the formation of quinone groups (Figure 5A). The metal salt was not used as a catalyst as it was reported elsewhere.^{24,25,40} The metallization reaction proceeded overnight and afterward the foils were extensively rinsed with water. To corroborate the gold metallization process, UV–vis spectra of PDOPA-modified substrates prior to and after immersion in HAuCl_4 solution were taken. Figure 5B shows the typical plasmonic absorption of gold colloids in those samples immersed overnight in the metallic precursor, thus confirming that gold reduction takes place in the presence of the PDOPA layer. I–V curves of metallized nanochannels exhibited a slight decrease in ionic current as a result of the metallization process that led to a decrease in the effective tip size (Figure 5C). However, no evidence of pore blocking was observed in different sets of experiments, which indicates that the PDOPA-mediated metallization occurs in a smooth fashion without disrupting/blocking the ion transport through the membrane.

Once the hybrid PDOPA/Au coating was obtained, we proceeded to functionalize the exposed gold surface with N,N,N -trimethyl(3-mercaptopropyl)ammonium chloride (NTMAC) in order to form a thiolate self-assembled monolayer (SAM) bearing quaternary ammonium groups. Self-assembled monolayers of NTMAC were created on

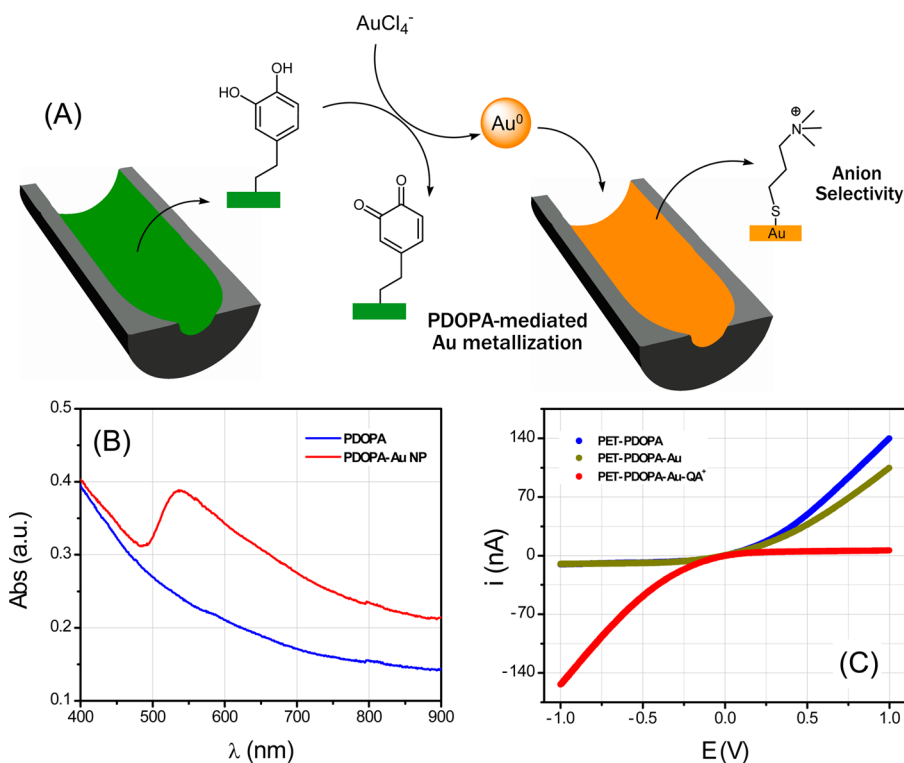


Figure 5. (A) Scheme describing the nanochannel metallization process mediated by PDOPA. The illustration shows the redox processes occurring on the pore walls when the metallic precursors are in contact with exposed catechol groups. (B) UV-vis spectra showing the plasmon absorption of gold after the metallization of PDOPA with HAuCl_4 precursors (red curve). The blue curve shows the UV-vis spectra of the PDOPA before the gold metallization. (C) I-V characteristics of a PDOPA-modified asymmetric nanochannel prior to (blue trace) and after (green trace) the metallization process. The red I-V plot describes the changes in the ion selectivity and rectification properties after the chemisorption of N,N,N -trimethyl(3-mercaptopropyl)ammonium chloride (NTMAC) self-assembled monolayers on metallized nanochannels. A reversion in the direction of the rectification is observed corresponding to a change in the sign of the surface charge.

PDOPA/Au-coated foils by immersing the substrates in a 10 mM ethanol solution at ambient conditions. In this example, surface modification was not only demonstrated by changes in surface wettability from 70° to 52° (see Supporting Information for details), upon assembling NTMAC on gold-modified membranes, but also by the reversal of the rectification properties due to the presence of positively charged terminal groups in the chemisorbed monolayer. I-V characterization of devices modified with NTMAC monolayers formed on the PDOPA/Au-coated nanochannels shows that the presence of the cationic SAM prompts a marked reversal of the rectification properties, thus changing f_{rec} from -10 to 25 after the chemisorption (Figure 5C, curve red). It is worth mentioning that Niu et al. have demonstrated that the main mechanism for the reaction between thiols and PDOPA after the formation of nanoparticles is the chemisorption of thiols on the metal particles and not a Michael addition of the thiols to PDOPA.⁴¹ These experiments reveal that the use of PDOPA-mediated surface processes can be extended to the metallization of asymmetric nanochannels without major disruption of their singular transport properties.

CONCLUSIONS

We reported here for the first time the integration of polydopamine into asymmetric single nanochannels to obtain highly functional chemical nanodevices. The proposed integrative concept is based on the chemical modification of nanofluidic devices by self-polymerization of dopamine and then use of the chemistry of polydopamine to carry out surface-

mediated secondary reactions. We demonstrate that the polymerization itself provides a way to adjust the dimensional characteristics of the nanochannel and improves the rectification of a nanofluidic diode, contributing as well to modification of the ionic transport properties of the nanodevice in a pH-dependent manner. We have shown that the presence of different functional groups facilitates the formation of positively or negatively charged pore surfaces under acidic or alkaline conditions, respectively, which in turn leads to the construction of nanofluidic devices with pH-reversible ion selectivity and rectification properties. Furthermore, it was shown that the PDOPA-coated nanochannel can be further modified by exploiting the chemical richness of the functional groups exposed on the PDOPA surface. Michael addition reaction was accomplished to graft ABA to the quinone groups in the PDOPA layer under mild conditions, thus resulting in the construction of nanochannels bearing primary amino groups. Protonation of these amino groups led to the formation of nanofluidic devices displaying anion-selective pH-controlled rectifying properties. In addition, by using the inherent reductive capacity of PDOPA, we demonstrated that catechol-mediated electroless reduction of gold can be performed on the pore walls to metallize the interior of the nanofluidic channel. Further modification with functional thiols confirmed that the formation of self-assembled monolayers on Au/PDOPA hybrids is feasible, thus opening the door to the powerful combination of self-assembly techniques and nanofluidic devices using highly robust and reproducible preparative protocols. We believe that the synergism arising from the

combination of the chemically versatile polydopamine “tool-box” and the remarkable physical characteristics of asymmetric nanopores offers a promising framework to explore new design concepts in nanofluidic devices.

■ ASSOCIATED CONTENT

Supporting Information

Wetting characterization of nanopore membranes. The Supporting Information is available free of charge on the ACS Publications website at DOI: 10.1021/jacs.5b01638.

■ AUTHOR INFORMATION

Corresponding Author

*E-mail: azzaroni@inifta.unlp.edu.ar.

Notes

The authors declare no competing financial interest.

■ ACKNOWLEDGMENTS

The authors acknowledge financial support from ANPCyT (PICT 2010-2554, PICT-2013-0905, and PPL 2011-003), Fundación Petruzza, and the Austrian Institute of Technology GmbH (AIT-CONICET Partner Lab: *Exploratory Research for Advanced Technologies in Supramolecular Materials Science* – Exp. 4947/11, Res. No. 3911, 28-12-2011) and from the Deutsche Forschungsgemeinschaft (DFG-FOR 1583). G.P.-M. and J.S.T. acknowledge CONICET for a doctoral and a postdoctoral fellowship, respectively. O.A. is a CONICET fellow.

■ REFERENCES

- (1) Daiguji, H. *Chem. Soc. Rev.* **2010**, *39*, 901–911.
- (2) Xu, H.; Wei, G.; Lei, J. *Chem. Soc. Rev.* **2011**, *40*, 2385–2401.
- (3) Choi, Y.; Baker, L. A.; Hillebrener, H.; Martin, C. R. *Phys. Chem. Chem. Phys.* **2006**, *8*, 4976–4988.
- (4) Wen, L.; Tian, Y.; Ma, J.; Zhai, J.; Jiang, L. *Phys. Chem. Chem. Phys.* **2012**, *14*, 4027–4042.
- (5) Tian, Y.; Wen, L.; Hou, X.; Hou, G.; Jiang, L. *ChemPhysChem* **2012**, *13*, 2455–2470.
- (6) Hou, X.; Zhang, H.; Jiang, L. *Angew. Chem., Int. Ed. Engl.* **2012**, *51*, 5296–5307.
- (7) Siwy, Z.; Heins, E.; Harrell, C. C.; Kohli, P.; Martin, C. R. *J. Am. Chem. Soc.* **2004**, *126*, 10850–10851.
- (8) (a) Sexton, L. T.; Horne, L. P.; Martin, C. R. *Mol. Biosyst.* **2007**, *3*, 667–685. (b) Siwy, Z. *Adv. Funct. Mater.* **2006**, *16*, 735–746. (c) Wei, C.; Bard, A. J.; Feldberg, S. W. *Anal. Chem.* **1997**, *69*, 4627–4633. (d) Siwy, Z.; Fulinski, A. *Phys. Rev. Lett.* **2002**, *89*, 198103-1–4.
- (9) (a) Cervera, J.; Schiedt, B.; Neumann, R.; Mafé, S.; Ramírez, P. J. *Chem. Phys.* **2006**, *124*, 104706-1–9. (b) Kosinska, I. D.; Goychuk, I.; Kostur, M.; Schmid, G.; Hänggi, P. *Phys. Rev. E* **2008**, *77*, 031131-1–10.
- (10) Siwy, Z.; Fulinski, A. *Am. J. Phys.* **2004**, *72*, 567–574.
- (11) Vlasiouk, I.; Kozel, T. R.; Siwy, Z. *J. Am. Chem. Soc.* **2009**, *131*, 8211–8220.
- (12) Siwy, Z.; Heins, E.; Harrell, C. C.; Kohli, P.; Martin, C. R. *J. Am. Chem. Soc.* **2004**, *126*, 10850–10851.
- (13) Hou, X.; Liu, Y. J.; Dong, H.; Yang, F.; Li, L.; Jiang, L. *Adv. Mater.* **2010**, *22*, 2440–2443.
- (14) (a) Hou, X.; Guo, W.; Xia, F.; Nie, F. Q.; Dong, H.; Tian, Y.; Wen, L. P.; Wang, L.; Cao, L. X.; Yang, Y.; Xue, J. M.; Song, Y. L.; Wang, Y. G.; Liu, D. S.; Jiang, L. *J. Am. Chem. Soc.* **2009**, *131*, 7800–7805. (b) Tian, Y.; Hou, X.; Wen, L. P.; Guo, W.; Song, Y. L.; Sun, H. Z.; Wang, Y. G.; Jiang, L.; Zhu, D. B. *Chem. Commun.* **2010**, *46*, 1682–1684.
- (15) (a) Yameen, B.; Ali, M.; Neumann, R.; Ensinger, W.; Knoll, W.; Azzaroni, A. *Small* **2009**, *5*, 1287. (b) Guo, W.; Xia, H. W.; Xia, F.; Hou, X.; Cao, L. X.; Wang, L.; Xue, J. M.; Zhang, G. Z.; Song, Y. L.; Zhu, D. B.; Wang, Y. G.; Jiang, L. *ChemPhysChem* **2010**, *11*, 859–864.
- (16) (a) Vlasiouk, I.; Kozel, T. R.; Siwy, Z. *J. Am. Chem. Soc.* **2009**, *131*, 8211–8220. (b) Han, X.; Hou, C. P.; Zhang, H. C.; Guo, W.; Li, H. B.; Jiang, L. *J. Am. Chem. Soc.* **2011**, *133*, 7644–7647. (c) Sun, Z. Y.; Han, C. P.; Wen, L.; Tian, D. M.; Li, H. B.; Jiang, L. *Chem. Commun.* **2012**, *48*, 3282–3284. (d) Li, S. J.; Li, J.; Wang, K.; Wang, C.; Xu, J. J.; Chen, H. Y.; Xia, X. H.; Huo, Q. *ACS Nano* **2010**, *4*, 6417–6424.
- (17) Guan, W. H.; Fan, R.; Reed, M. A. *Nat. Commun.* **2011**, *2*, 506.
- (18) Lan, W. J.; Holden, D. A.; White, H. S. *J. Am. Chem. Soc.* **2011**, *133*, 13300–13303.
- (19) Zhang, M.; Meng, Z.; Zhai, J.; Jiang, L. *Chem. Commun.* **2013**, *49*, 2284–2286.
- (20) Lee, H.; Dellatore, S. M.; Miller, W. M.; Messersmith, P. B. *Science* **2007**, *318*, 426–430.
- (21) Lee, H.; Rho, J.; Messersmith, P. B. *Adv. Mater.* **2009**, *21*, 431–434.
- (22) Schaubroeck, D.; Vercammen, Y.; Van Vaeck, L.; Vanderleyden, E.; Dubrueel, P.; Vanfleteren, J. *Appl. Surf. Sci.* **2014**, *303*, 465–472.
- (23) Cao, Y.; Zhang, Y.; Tao, L.; Li, K.; Xue, Z.; Feng, L.; Wei, Y. *ACS Appl. Mater. Interfaces* **2013**, *5*, 4438–4442.
- (24) Xu, H.; Liu, X.; Su, G.; Zhang, B.; Wang, D. *Langmuir* **2012**, *28*, 13060.
- (25) Baron, R.; Zayat, M.; Willner, I. *Anal. Chem.* **2005**, *77*, 1566–1571.
- (26) Tien, J.; Terfort, A.; Whitesides, G. M. *Langmuir* **1997**, *13*, 5349–5355.
- (27) Apel, P. Yu.; Blonskaya, I. V.; Dmitriev, S. N.; Orelovitch, O. L.; Presz, A.; Sartowska, B. A. *Nanotechnology* **2007**, *18*, 305302.
- (28) Apel, P. Yu.; Blonskaya, I. V.; Levkovich, N. V.; Orelovitch, O. L. *Pet. Chem.* **2011**, *51*, 555–567.
- (29) Apel, P. Yu.; Blonskaya, I. V.; Orelovitch, O. L.; Ramirez, P.; Sartowska, B. A. *Nanotechnology* **2011**, *22*, 175302.
- (30) Apel, P. Yu.; Korchev, Yu. E.; Siwy, Z.; Spohr, R.; Yoshida, M. *Nucl. Instrum. Methods Phys. Res., Sect. B* **2001**, *184*, 337–346.
- (31) Trautmann, C.; Briichle, W.; Spohr, R.; Vetter, J.; Angert, N. *Nucl. Instrum. Methods Phys. Res., Sect. B* **1996**, *111*, 70–74.
- (32) Harrell, C. C.; Siwy, Z.; Martin, C. R. *Small* **2006**, *2*, 194–198.
- (33) Apel, P. Yu.; Blonskaya, I. V.; Cornelius, T. W.; Neumann, R.; Spohr, R.; Schwartz, K.; Skuratov, V. A.; Trautmann, C. *Radiat. Meas.* **2009**, *44*, 759–762.
- (34) Yu, B.; Liu, J.; Liu, S.; Zhou, F. *Chem. Commun.* **2010**, *46*, 5900–5902.
- (35) Bernsmann, F.; Frisch, B.; Ringwald, C.; Ball, V. *J. Colloid Interface Sci.* **2010**, *344*, 54–60.
- (36) Ball, V.; Gracio, J.; Vila, M.; Singh, M. K.; Metz-Boutigue, M. H.; Michel, M.; Bour, J.; Toniazzi, V.; Ruch, D.; Buehler, M. J. *Langmuir* **2013**, *29*, 12754–12761.
- (37) Tagliazucchi, M.; Azzaroni, O.; Szeleifer, I. *J. Am. Chem. Soc.* **2010**, *132*, 12404–12411.
- (38) (a) Hou, X.; Dong, H.; Zhu, D.; Jiang, L. *Small* **2010**, *6*, 361–365. (b) Tian, Y.; Hou, X.; Jiang, L. *J. Electroanal. Chem.* **2011**, *656*, 231–236.
- (39) (a) Baker, L. a.; Jin, P.; Martin, C. R. *Crit. Rev. Solid State Mater. Sci.* **2005**, *30*, 183–205. (b) Wirtz, M.; Parker, M.; Kobayashi, Y.; Martin, C. R. *Chem. Rec.* **2002**, *2*, 259–267. (c) Martin, C. R. *Science* **1994**, *266*, 1961–1966.
- (40) Fu, Y.; Li, P.; Xie, Q.; Xu, X.; Lei, L.; Chen, C.; Zou, C.; Deng, W.; Yao, S. *Adv. Funct. Mater.* **2009**, *19*, 1784–1791.
- (41) Niu, H.; Wang, S.; Zeng, T.; Wang, Y.; Zhang, X.; Meng, Z.; Cai, Y. *J. Mater. Chem.* **2012**, *22*, 15644.